BEILSTEIN JOURNAL OF NANOTECHNOLOGY

Supporting Information

for

Optimization of NiMo alloy nanoparticles for catalytic dry reforming of methane

Azimet A. Karluk, Javeed Mahmood, Seok-Jin Kim and Cafer T. Yavuz

Beilstein J. Nanotechnol. **2026,** *17,* 1212–1222. doi:10.3762/bjnano.17.84

Additional figures and table

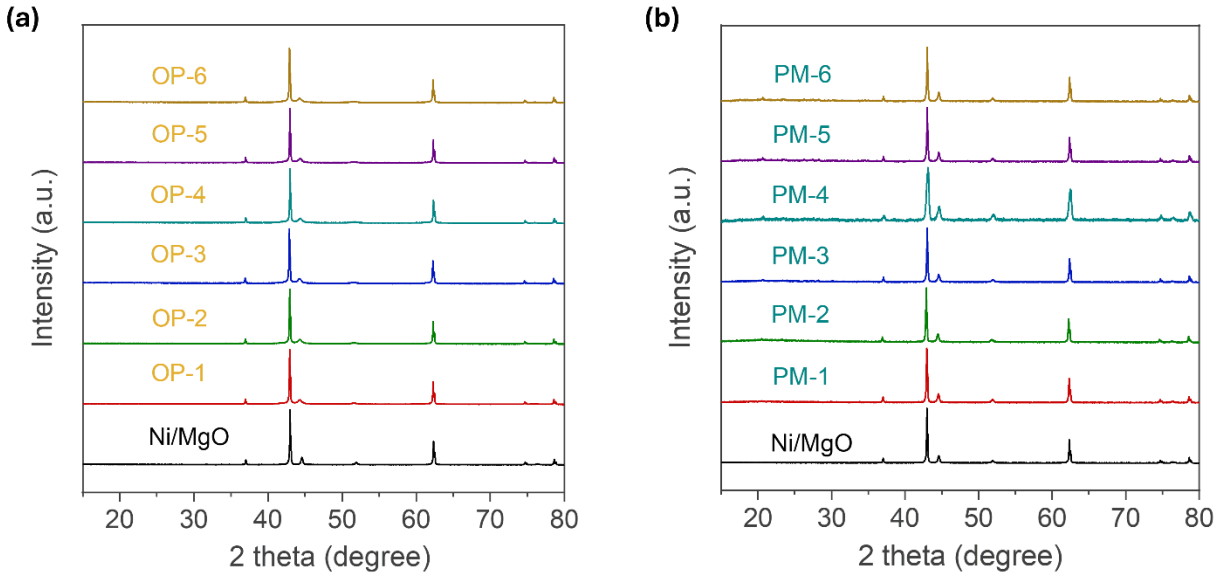

Figure S1: Powder XRD patterns of (a) OP-*x* and (b) PM-*x*, before DRM reaction.

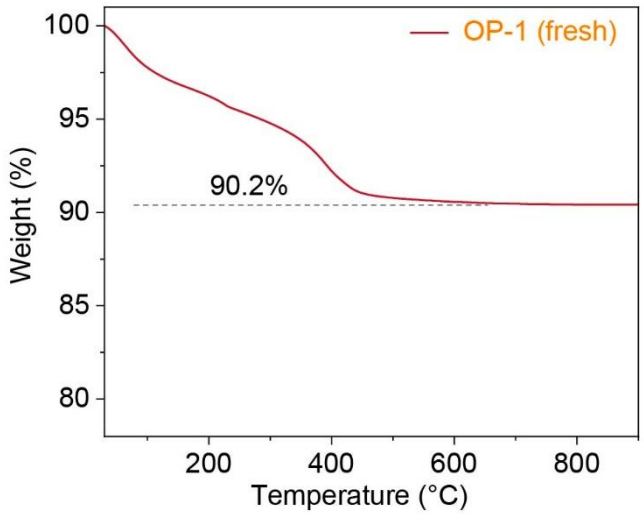

Figure S2: Thermogravimetric analysis (TGA) profile of fresh OP-1 recorded under N_2 flow (20 mL·min^{-1}), with a heating rate of 10 °C·min^{-1}. The total weight loss of ≈9.8 wt % is attributed to the removal of adsorbed species and decomposition of residual surface functionalities.

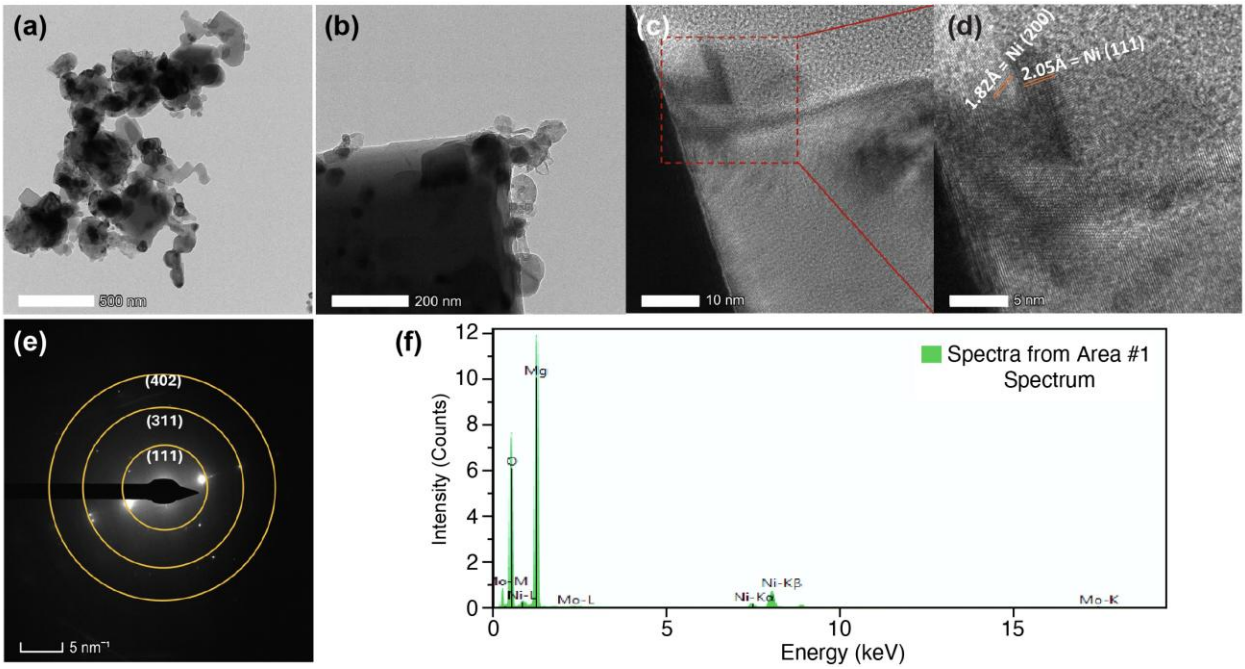

Figure S3: (a-b) TEM images, (c-d) High resolution TEM (HR-TEM) images, (e) Selected area electron diffraction (SAED) pattern, and (f) energy-dispersive X-ray (EDX) spectra of OP-2. The HR-TEM image reveals clear lattice fringes consistent with the SAED patterns. EDS confirms the elemental composition of the sample.

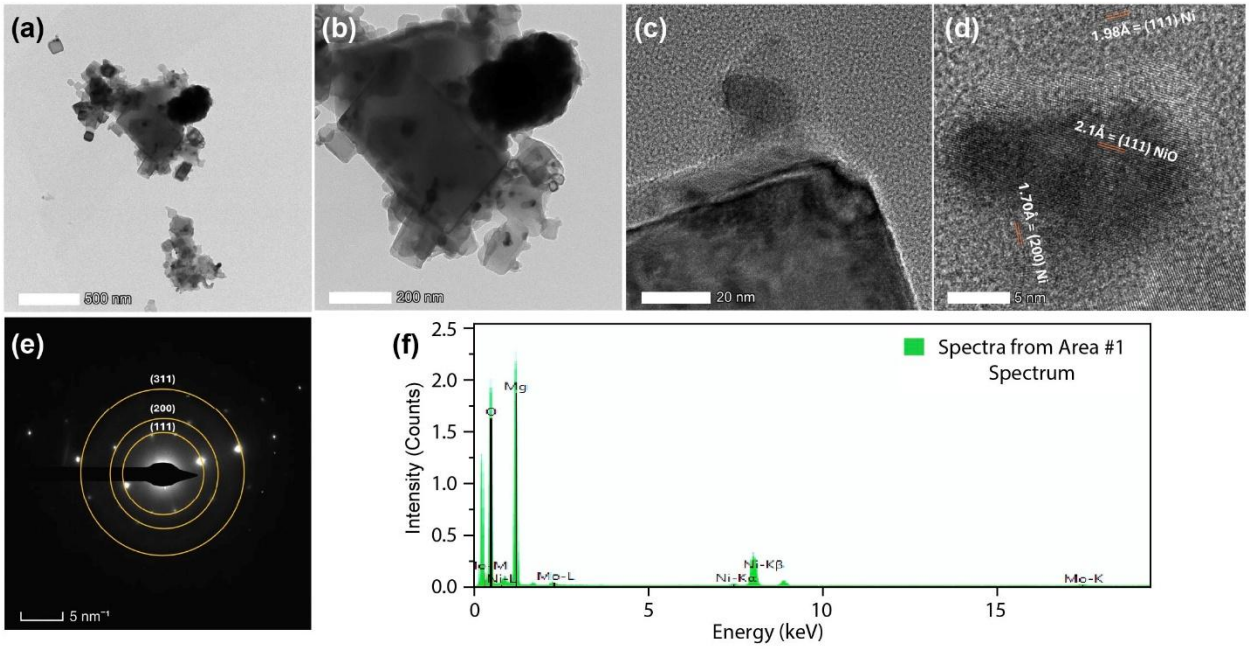

Figure S4: (a-b) TEM images, (c-d) High resolution TEM (HR-TEM) images, (e) Selected area electron diffraction (SAED) pattern, and (f) Energy-dispersive X-ray (EDX) spectra of PM-2. The HR-TEM image reveals clear lattice fringes consistent with the SAED patterns. EDS confirms the elemental composition of the sample.

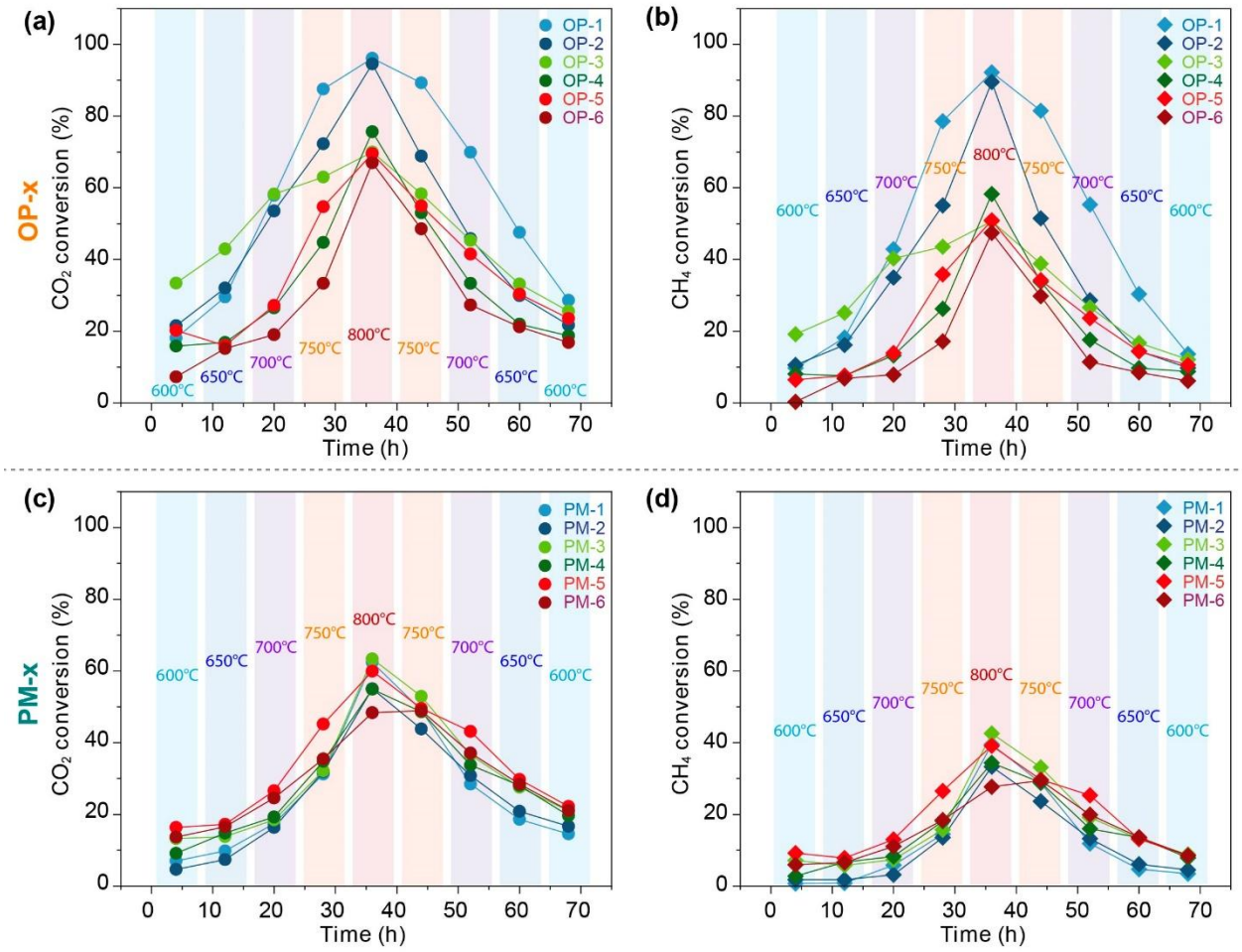

Figure S5: CO_2 and CH_4 conversions of (a-b) OP-*x* and (c-d) PM-*x* at different temperatures (Reaction conditions: 1 bar, 25 mg OP-*x* or PM-*x*, $CH_4/CO_2/N_2$ = 2:2:6, weight hourly space velocity (WHSV) = 25,680 $mL \cdot g^{-1} \cdot h^{-1}$).

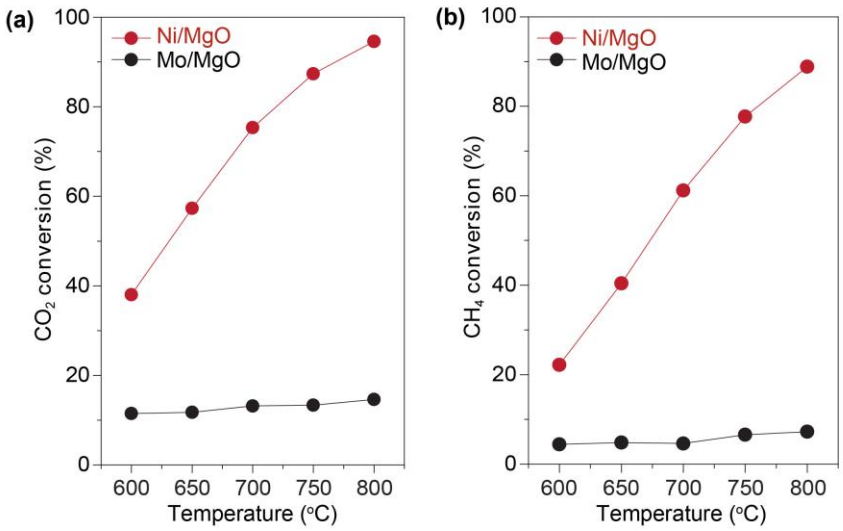

Figure S6: Comparison of CO_2 (a) and CH_4 conversions (b) of only Ni and only Mo on MgO at different temperatures (Reaction conditions: 1 bar, 25 mg, $CH_4/CO_2/N_2$ = 2:2:6, weight hourly space velocity (WHSV) = 25,680 $mL \cdot g^{-1} \cdot h^{-1}$).

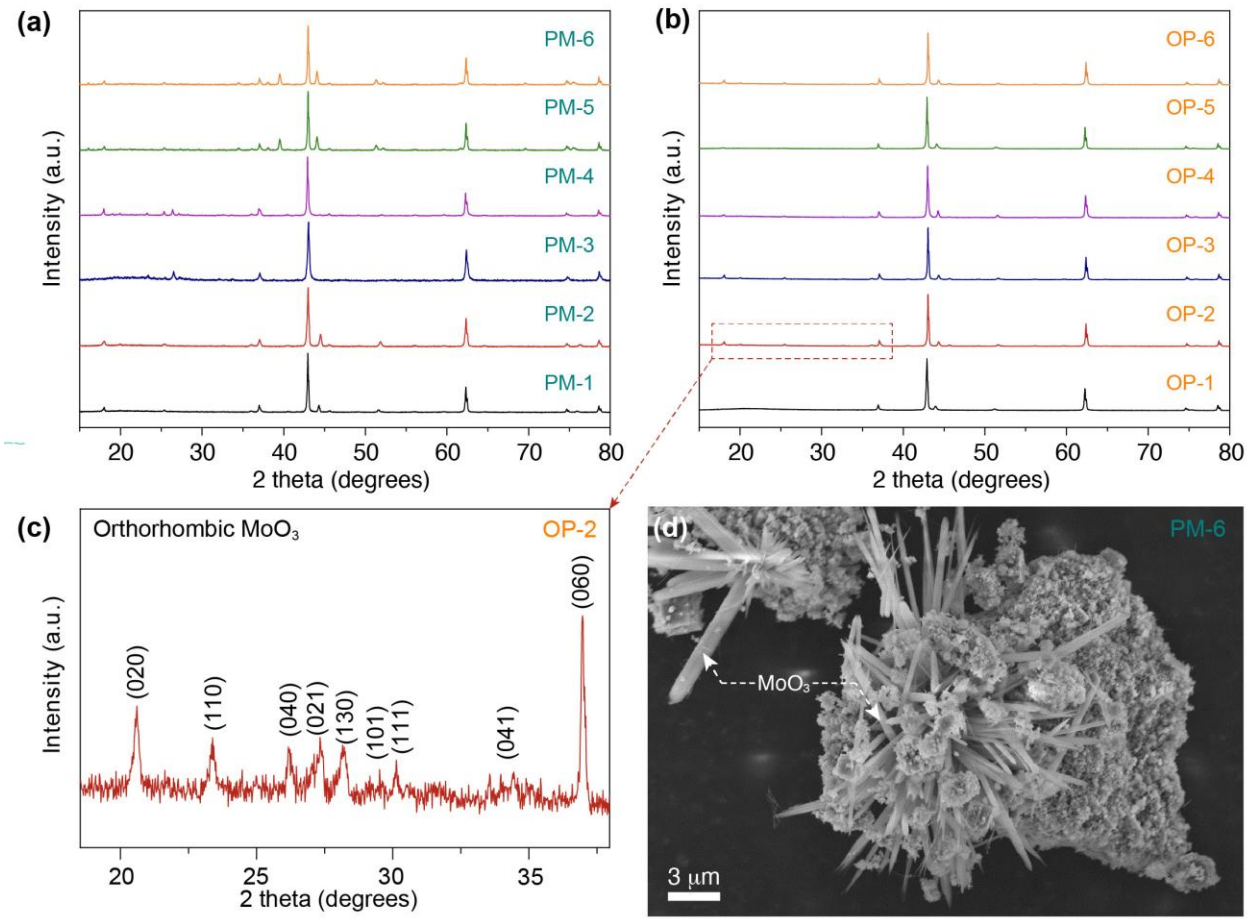

Figure S7: PXRD patterns of (a) PM-*x* before DRM and (b) OP-*x* samples after DRM reaction; (c) Enlarged XRD patterns which indicate the orthorhombic phase of MoO_3 (JCPDS-05-0508) crystal from OP-2; (d) SEM images of PM-6 after DRM reaction.

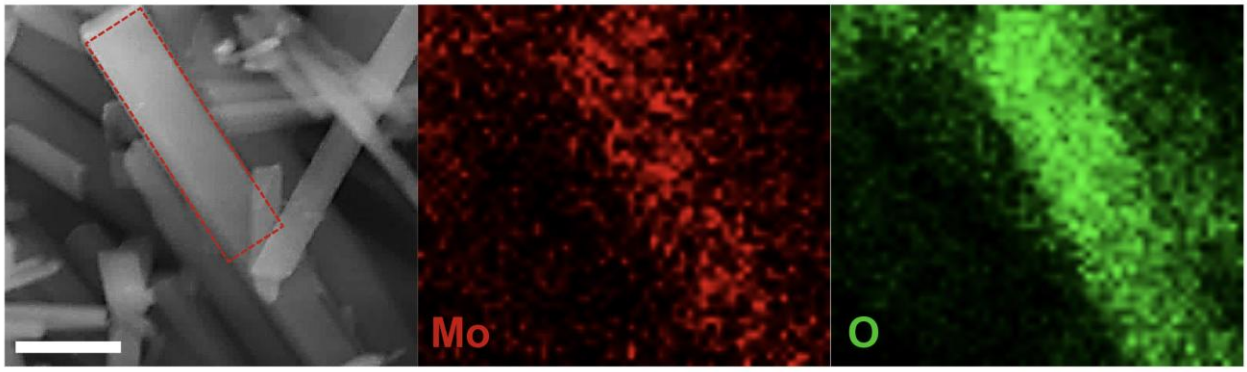

Figure S8: SEM image of rod-shaped MoO_3 crystal and EDS map for PM-6 (Scale bar: 1 μm, Red: Mo, Green: O).

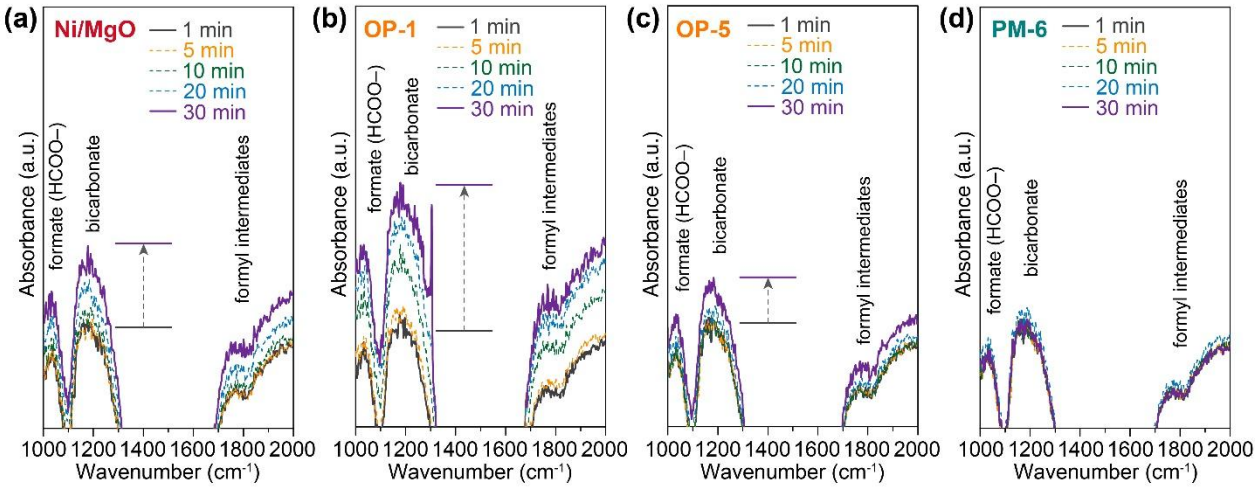

Figure S9: In situ DRIFT spectra collected during CO_2 reduction at 750 °C on Ni/MgO, OP-1, OP-5, and PM-6, respectively. The spectra were acquired sequentially under pure CO_2 flow (99.999%, 10 mL·min^{-1}, 30 min) followed by pure H_2 flow (99.999%, 10 mL·min^{-1}, 30 min).

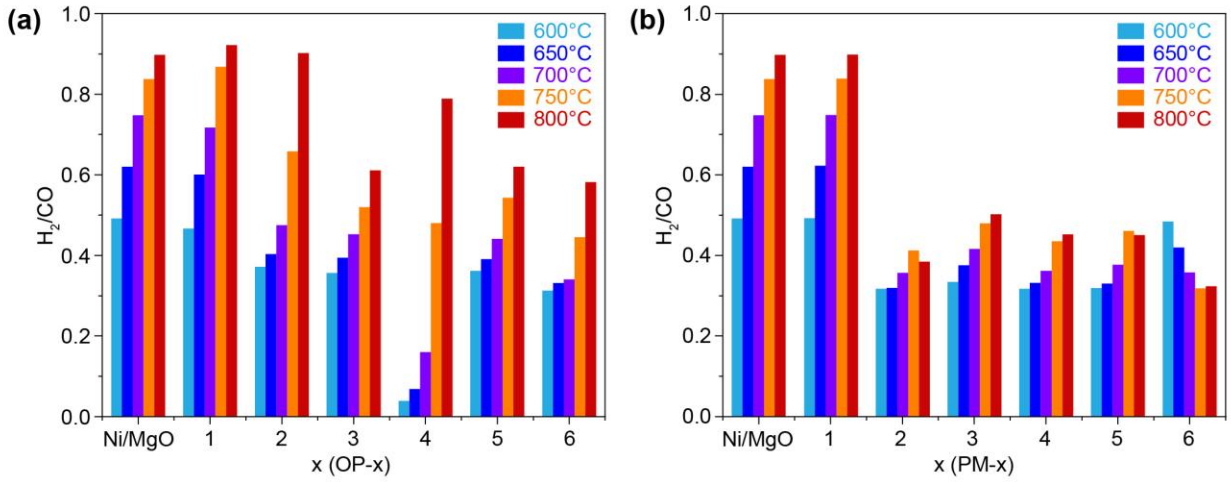

Figure S10: H_2 to CO ratios of OP-*x* samples (a) and PM-*x* samples (b) at different temperatures from 600 to 800 °C (Reaction conditions: 1 bar, 25 mg OP-*x* or (PM-*x*), $CH_4/CO_2/N_2$ = 2:2:6, Weight hourly space velocity (WHSV): 25,680 $mL \cdot g^{-1} \cdot h^{-1}$).

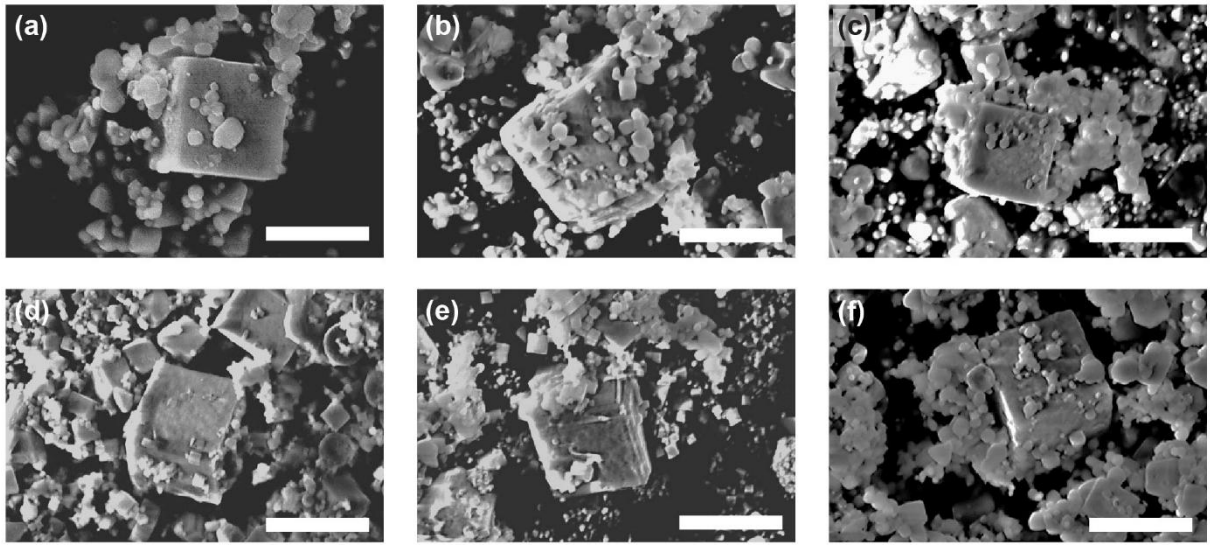

Figure S11: SEM images of OP-*x* (*x* = 1–6) before DRM (scale bar 1 μm). OP-1 to 6 all represent (a), (b), (c), (d), (e), and (f) in that order.

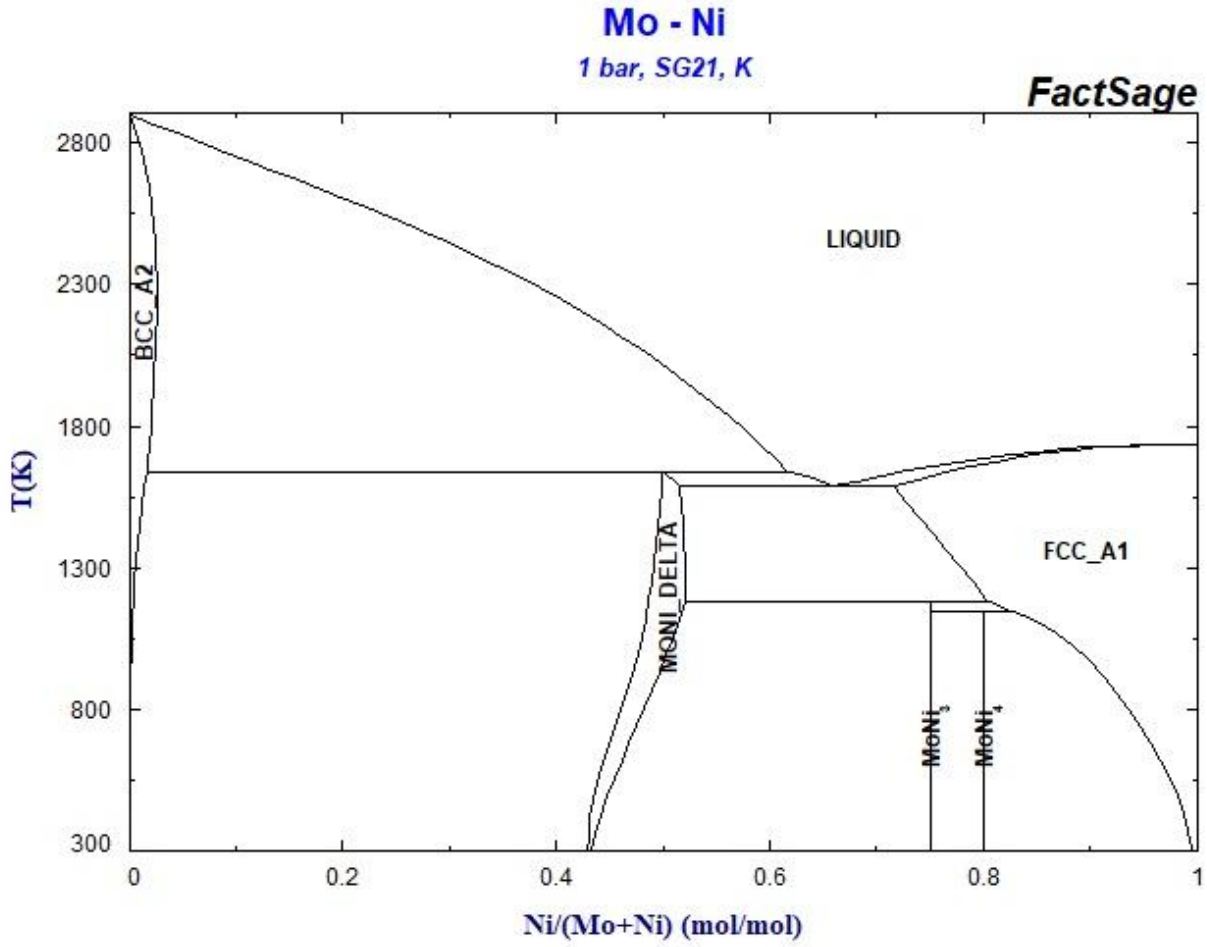

Figure S12: Alloy phase diagrams of Ni-Mo, from FactSage® [1] thermochemical values collection on SGTE 2022 alloy database, https://www.crct.polymtl.ca/fact/phase_diagram.php?file=Mo-Ni.jpg&dir=SGTE2022.

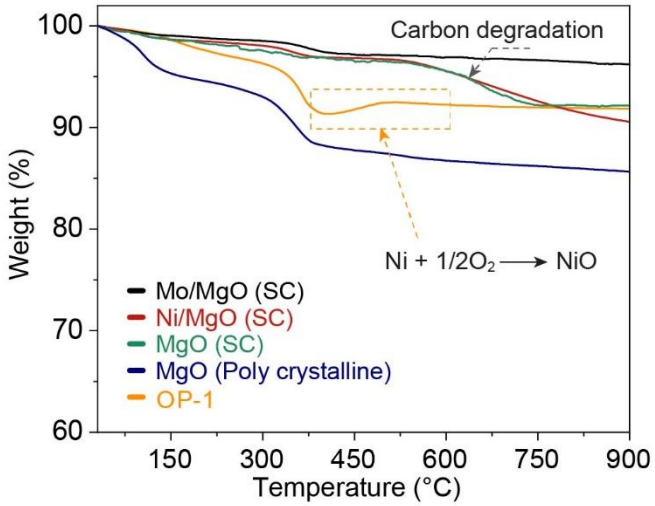

Figure S13: TGA analysis of Ni/MgO (single crystalline, SC), Mo/MgO (SC), MgO (SC), and polycrystalline MgO was conducted under air flow with a temperature ramp of 10 °C·min^{-1}. Samples were analyzed after exposure to harsh DRM conditions (10 mL·min^{-1} of CH_4 and CO_2 flow, no inert gas, for 48 hours at 800 °C).

Table S1: ICP-OES analysis results of OP-*x* and PM-*x* samples. The table lists the expected Ni and Mo loadings (wt %), together with the actual metal contents measured for catalysts synthesized *via* the one-pot (OP) method and after post-modification (PM).

Catalysts	Expected metal loading (wt %)		One-pot synthesis (OP) ICP (wt %)		Post-modification (PM) ICP (wt %)	
	Ni	Mo	Ni	Mo	Ni	Mo
NiMo-1	8.80	1.75	7.01	1.14	6.79	1.61
NiMo-2	8.63	3.45	6.70	1.30	6.67	2.98
NiMo-3	8.47	5.08	6.69	1.60	6.48	5.01
NiMo-4	8.31	6.66	5.80	2.40	6.32	6.51
NiMo-5	8.16	8.24	5.70	2.68	6.30	7.62
NiMo-6	8.02	9.63	5.04	2.83	6.27	8.80

Reference

1. Bale, C. W.; Chartrand, P.; Degterov, S.; Eriksson, G.; Hack, K.; Mahfoud, R. B.; Melançon, J.; Pelton, A.; Petersen, S. *Calphad* **2002**, *26* (2), 189-228.